Plasma parameters in a planar dc magnetron sputtering discharge of argon and krypton

P. Sigurjonsson and J. T. Gudmundsson

Science Institute, University of Iceland, Reykjavik, Iceland
Department of Electrical Engineering, University of Iceland, Reykjavik, Iceland
tumi@hi.is

Introduction

- A typical dc planar magnetron sputtering discharge operates at a pressure of 1 – 10 mTorr with a magnetic field strength of 0.01 – 0.05 T and cathode potentials 300 – 700 V (Waits, 1978).
- Electron energy distribution functions (EEDF) in dc magnetron sputtering discharge are generally found to be either Maxwellian like or bi-Maxwellian like in nature, depending on pressure and spatial location (Sheridan et al., 1991; Seo et al., 2004).
- Maxwellian like electron energy distributions are found in or near the magnetic trap and bi-Maxwellian like distributions are found further away from the cathode target (Sheridan et al., 1991).
- The electron temperature and electron density are known to decrease with distance from the cathode target (Rossnagel and Kaufman, 1986).
- Outside the magnetic trap the plasma potential is generally found to have a weak dependence on spatial location and pressure (Sheridan et al., 1991; Field et al., 2002).
- Here we explore the spatial dependence of the:
  - electron energy distribution function (EEDF)
  - electron density
  - electron temperature
  - plasma potential

  in the substrate vicinity.
- A comparison is made between argon and krypton sputtering gas.

Experimental apparatus

- A standard planar magnetron source was operated with a 76.2 mm diameter copper (Cu) target inside a stainless steel chamber, 200 mm in diameter and 250 mm long.
- The magnetron is operated in a constant power mode at 100 W. The target voltage was in the range 380 ± 5 V to 450 ± 5 V, and the target current was from 220 ± 15 mA to 250 ± 10 mA.
- Argon (Ar) and Krypton (Kr) of purity 99.9997 %, were used as discharge gases at four different pressures 3, 5, 10 and 15 mTorr.
- The Langmuir probe current-voltage characteristic was recorded.
- The second derivative was obtained by numerically differentiating and filtering (Magnus and Gudmundsson, 2002) the measured curve to determine the electron energy distribution function (EEDF) from Druyvesteyn formula (Lieberman and Lichtenberg, 2005, p. 191).
- The electron density was found by

$$n_e = \int_0^\infty g_e(\mathcal{E})d\mathcal{E} \tag{1}$$

Results and discussion

- Two groups of electrons are apparent for both argon and krypton discharge.
- For both groups the electron temperature decreases with increased distance from the cathode target.
- The electron temperature of the cold electrons is roughly independent of the discharge pressure, while the electron temperature of the hot electrons decreases with increased discharge pressure.
- The plasma potential is in the range 1.4 – 1.8 V for an argon discharge and in the range 1.35 – 2.2 V for a krypton discharge and is spatially uniform outside the magnetic trap in the range 20 – 120 mm and increases with increased discharge pressure.
- The bi-Maxwellian like EEDF is commonly observed in the substrate vicinity in magnetron sputtering discharges (Sheridan et al., 1991; Seo et al., 2004; Seo and Chang, 2004).
- The hot electrons are created in the magnetic trap in the cathode fall regions and drift to the downstream region under the influence of a diverging magnetic field (Rossnagel and Kaufman, 1986; Seo and Chang, 2004).
- The low and flat distribution of the plasma potential traps the cold electrons in the substrate vicinity.
- Thus, a bi-Maxwellian like electron energy distribution is observed in the downstream region.

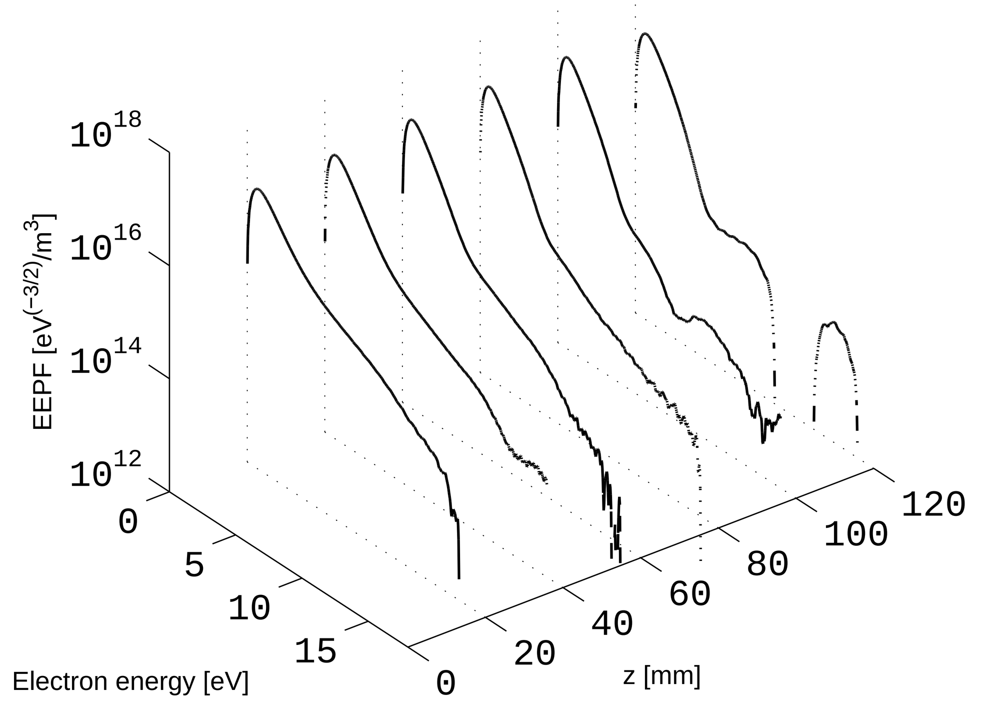

Figure 1: The electron energy probability function (EEPF) along the discharge center axis for argon discharge at 5 mTorr.

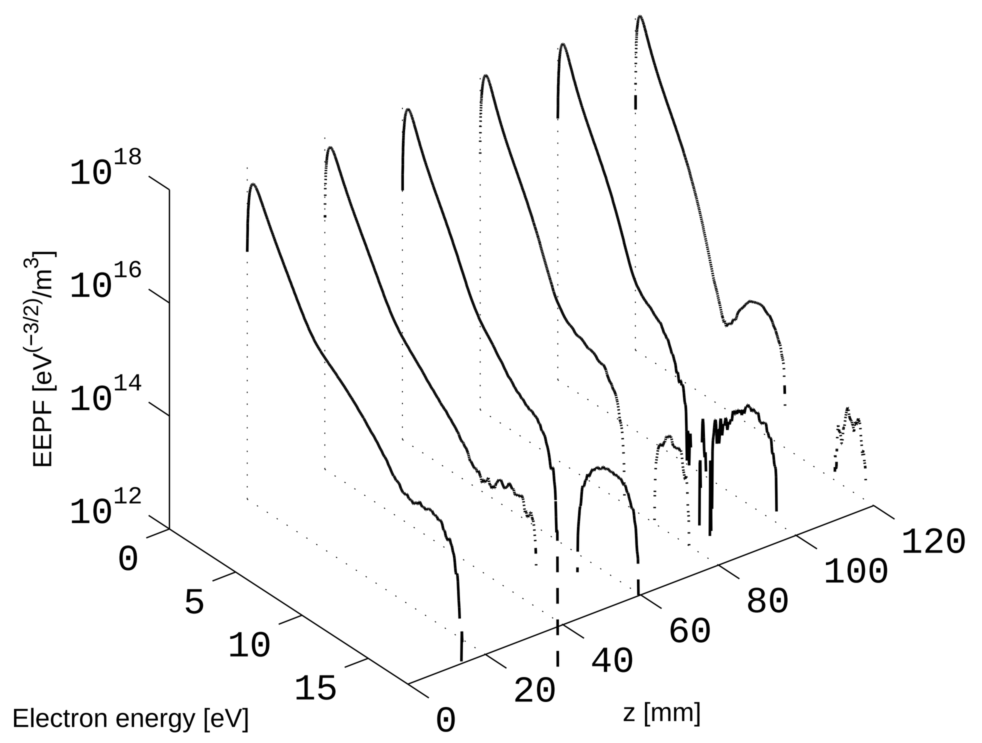

Figure 2: The electron energy probability function (EEPF) along the discharge center axis for krypton discharge at 5 mTorr.

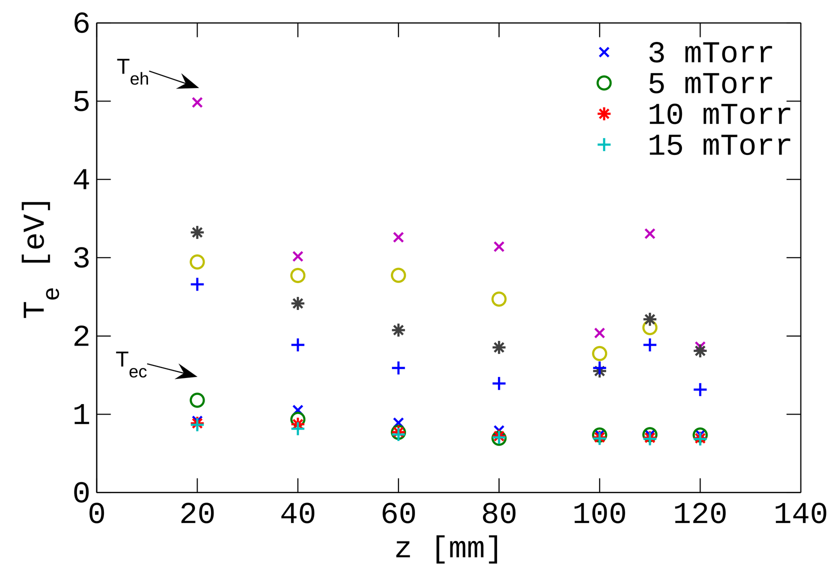

Figure 3: The electron temperature for hot electrons T_{eh} and cold electrons T_{ec} versus distance from the target along the discharge center axis for argon discharge.

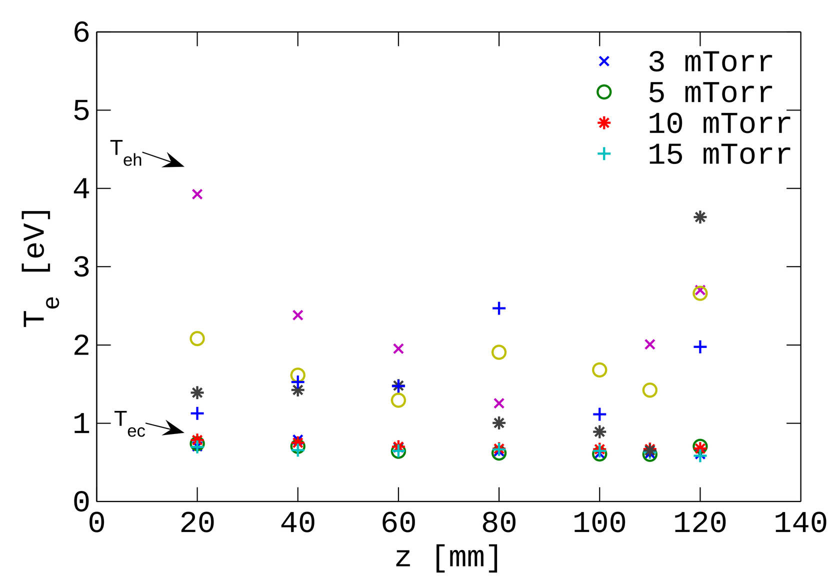

Figure 4: The electron temperature for hot electrons T_{eh} and cold electrons T_{ec} versus distance from the target along the discharge center axis for krypton discharge.

- The electron density in a krypton discharge is roughly a factor of 2 – 3 higher than for an argon discharge.
- Higher electron density is expected in a krypton discharge than for an argon discharge since the ratio of electron impact ionization rate coefficient $k_{iz,Kr}/k_{iz,Ar} \approx 2.9$ for electron temperature of 2 eV and 2.2 for electron temperature of 3 eV (Kannari et al., 1985).

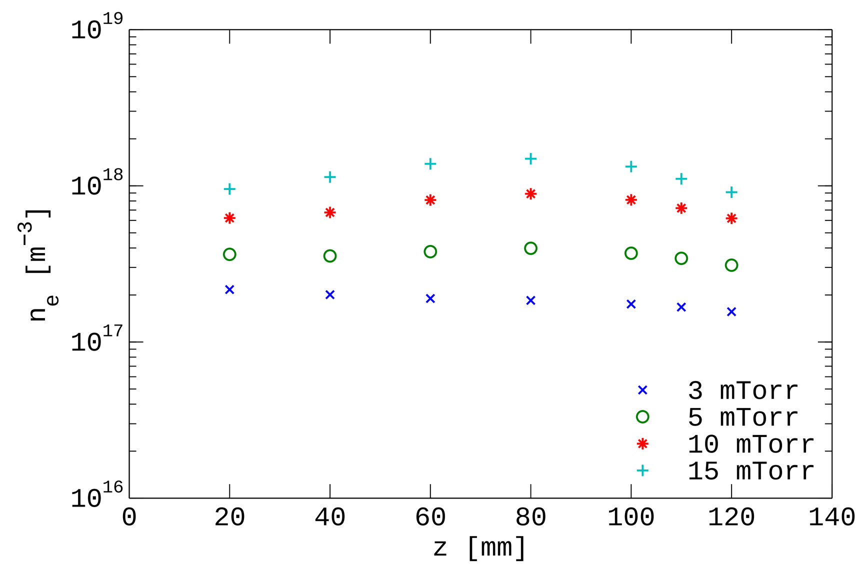

Figure 5: The electron density versus distance from the target along the discharge center axis for argon discharge.

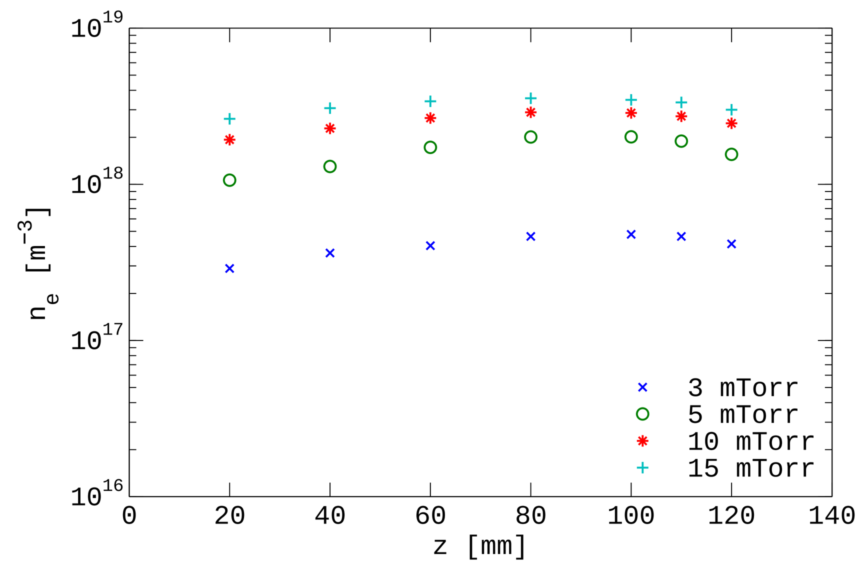

Figure 6: The electron density versus distance from the target along the discharge center axis for krypton discharge.

Conclusions

- Two groups of electrons are observed in the discharge.
- The electron temperature of the cold electrons is roughly independent of the discharge pressure, while the electron temperature of the hot electrons decreases with increased discharge pressure.
- The electron density increases with increased pressure and is roughly a factor of 2 – 3 higher for a krypton discharge than for an argon discharge.

Acknowledgments

This work was partially supported by the Icelandic Student Innovation Fund, the Icelandic Research Fund, and the University of Iceland Research Fund.

References

D. J. Field, S. K. Dew, and R. E. Burrell, Journal of Vacuum Science and Technology A **20**, 2032 (2002).

F. Kannari, M. Obara, and T. Fujioka, Journal of Applied Physics **57**, 4309 (1985).

M. A. Lieberman and A. J. Lichtenberg, *Principles of Plasma Discharges and Materials Processing* (John Wiley & Sons, New York, 2005), 2nd ed.

F. Magnus and J. T. Gudmundsson, *Digital smoothing of the I – V Langmuir probe characteristic*, Technical Report RH-20-02, Science Institute, University of Iceland (2002).

S. M. Rossnagel and H. R. Kaufman, Journal of Vacuum Science and Technology A **4**, 1822 (1986).

S.-H. Seo and H.-Y. Chang, Journal of Applied Physics **96**, 1310 (2004).

S.-H. Seo, J.-H. In, and H.-Y. Chang, Plasma Sources Science and Technology **13**, 409 (2004).

T. E. Sheridan, M. J. Goeckner, and J. Goree, Journal of Vacuum Science and Technology A **9**, 688 (1991).

R. K. Waits, Journal of Vacuum Science and Technology **15**, 179 (1978).